Assessing the Webb-Pearman-Leuning Formula in Estimating CO_2 Flux at a Tropical Coast

Muhammad Fikri Sigid [1,*], Yusri Yusup [1,2], Abdulghani Essayah Swesi [1], Haitem M Almdhun [1], and Ehsan Jolous Jamshidi [1]

[1] Environmental Technology, School of Industrial Technology, Universiti Sains Malaysia, USM 11800, Pulau Pinang, Malaysia.

[2] Centre for Marine & Coastal Studies (CEMACS), Universiti Sains Malaysia, Pulau Pinang, Malaysia.

Corresponding author: Yusri Yusup (yusriy@usm.my)

Key Points:

- The Webb-Pearman-Leuning formula improves CO_2 flux measurement accuracy in tropical coastal waters using eddy covariance method.
- The Webb-Pearman-Leuning correction produces a lower magnitude flux than the uncorrected CO_2 flux, minimizing the CO_2 flux overestimation.
- The Webb-Pearman-Leuning correction can alter the sign of CO_2 flux, emphasizing the conscientious implementation of the formula.

Abstract

The Webb-Pearman-Leuning (WPL) formula is used to minimize the overestimate CO_2 flux by open-path gas analyzer and eddy covariance methods. However, its effectiveness for tropical coastal waters with high air water vapor content requires investigation. This paper assesses the WPL correction on CO_2 flux measurement over the tropical coastal water using three calculation methods: standard (including WPL and other correction methods), raw, and WPL. The results showed that the standard method yielded CO_2 flux of –0.10 μmol m^{-2} s^{-1}, which is 60% lower than the raw. The WPL-CO_2 flux (–0.07 μmol m^{-2} s^{-1}) is also lower than the raw (–0.25 μmol m^{-2} s^{-1}) by 0.17 μmol m^{-2} s^{-1}. The WPL formula serves its purpose in minimizing the CO_2 flux overestimation but uses caution with the formula as it can change positive-negative flux signs, especially with temperature and water vapor corrections.

Plain Language Summary

The Webb-Pearman-Leuning (WPL) formula is a method used to correct overestimation of CO_2 flux when measuring gas and wind patterns in the air. It has been found to work well in some areas, but we need to investigate how well it works in tropical coastal waters where the air is very humid. This study looked at how well the WPL formula works in three different ways of calculating CO_2 flux: the standard way (which uses WPL and other methods), the raw way (which doesn't use WPL), and the WPL way. The results showed that the standard way gave a CO_2 flux of –0.10 μmol m^{-2} s^{-1}, which is 60% lower than the raw way. The WPL way gave a CO_2 flux of –0.07 μmol m^{-2} s^{-1}, which is lower than the raw way by 0.17 μmol m^{-2} s^{-1}. The WPL formula is good at correcting overestimation, but we need to be careful when using it, especially when correcting for temperature and humidity, because it can change whether the CO_2 flux is positive or negative.

1. Introduction

Carbon dioxide (CO_2) fluxes can be directly estimated using the eddy covariance (EC) technique (Burba et al., 2013). The EC method is often used by ecosystem researchers because it has the advantage of quantifying mass (e.g., CO_2, methane, water, etc.) and energy (sensible and latent heat) exchanges of expansive areas, such as forests, croplands, and oceans (Chien et al., 2018; Heimsch et al., 2021; Lokupitiya et al., 2016; Nakai et al., 2008; Tokoro & Kuwae, 2018).

The EC method uses the understanding of the behavior of turbulent eddies and utilizes vertical turbulent exchange principles to calculate the flux using the covariance of the high-frequency mixing ratio of CO_2 or moisture and the vertical velocity component of the wind (McGowan et al., 2016; Stull, 1988). High-frequency measurements of wind velocity components are afforded by sonic anemometers, but the measurement of CO_2 or moisture (H_2O) mixing ratio requires fast-response analyzers. The Infrared Gas Analyzers (IRGA) was developed to measure CO_2 or H_2O mixing ratios at high frequencies (e.g., 10 or 20 Hz). At high frequencies, the rapid-response analyzer could capture turbulent exchange and be able to satisfy the EC method requirement (Jones & Smith, 1977).

The first type of IRGA that measure CO_2 flux on the ocean was the open-path gas analyzer, and research conducted in the last few decades demonstrated the widespread use of the analyzer in air-sea CO_2 flux studies (Yang et al., 2016). However, previous studies have shown that the use of open-path gas analyzer can result in the overestimation of the CO_2 flux due to the effects of water vapor and temperature (Broecker et al., 1986; Edson et al., 2011; Else et al., 2011; Prytherch, Yelland, Pascal, Moat, Skjelvan, & Srokosz, 2010). To minimize the error in the calculated flux, the correction method of the Webb-Pearman-Leuning (WPL) was developed. The WPL formulation was developed to eliminate the effects of air density fluctuations on the molar density of CO_2 that could occur in the open-path systems (Burba et al., 2008; Miller et al., 2010). Webb et al. (1980) proposed the correction by using a formula that considers air density generated by water vapor and latent heat. Variables of temperature, pressure, and molar density were calculated by the formula to produce the corrected CO_2 flux from the gas analyzer.

On top of the WPL correction, other corrections are applied to the raw CO_2 flux estimated: 1) wind speed measurement offsets and 2) flux spectral corrections. The offset is necessary because wind speed readings from a sonic anemometer can be inaccurate because of the measurement drift (LI-COR, 2021). The spectral corrections are applied to compensate underestimation of fluxes: 1) the low-pass filtering correction for flux losses due to turbulence fluctuation dampening, and 2) the high-pass filtering correction for flux losses caused by long-term turbulent effects due to the finite averaging time of fluxes (LI-COR, 2021). The procedures of low-pass filtering correction are utilized to correct flux spectral properties and describe flux attenuations due to the imperfect instrumental setup (Moncrieff et al., 1997). The process involves estimating the true co-spectra, determining a low-pass transfer function, and applying the function to the estimated true flux co-spectrum so that a high-frequency flux attenuation can be obtained. In addition, the high-frequency spectral correction performs a simple correction formula based on first-order filters and analytical co-spectra formulation for high-frequency spectral losses and flux co-spectra (Horst, 1997; Massman, 2000, 2001; Moncrieff et al., 1997).

Some researchers reported that the coastal region is a weak carbon source or uptake (Borges et al., 2005). The net CO_2 flux measured in northwestern Taiwan was -1.75 ± 0.98 µmol m^{-2} s^{-1}, with the diurnal flux influenced by local wind speed. Similarly, in Todos Santos Bay, Mexico, the CO_2 flux was -1.32 ± 8.94 µmol m^{-2} s^{-1} (Gutiérrez-Loza & Ocampo-Torres, 2016). The CO_2 flux at Bodega Bay, California, was also a weak source, with 0.39 ± 1.84 µmol m^{-2} s^{-1} during the upwelling period and 0.05 ± 0.79 µmol m^{-2} s^{-1} during the relaxation period (Ikawa et al., 2013). Despite their importance, there is still notable uncertainty in how to parameterize these fluxes for global climate models, and more observations are necessary to gain a better understanding of the role of coastal seas in the global carbon cycle (Chien et al., 2018; Doney et al., 2009; Gutiérrez-Loza & Ocampo-Torres, 2016). Additionally, measuring these fluxes using techniques and corrections is challenging because of the high uncertainties introduced during data processing, especially for smaller fluxes (Else et al., 2011; Prytherch, Yelland, Pascal, Moat, Skjelvan, & Neill, 2010). Coastal waters can display high variability in CO_2 flux due to various factors, such as water temperature, salinity, and biological activity (Ikawa et al., 2013). Despite this, wind speed plays a critical role in controlling the magnitude of air-sea CO_2 exchanges, and low wind speeds can restrict gas transfer, resulting in reduced CO_2 fluxes in some cases (Aalto et al., 2021). The flux over the coast is low compared to fluxes on land (He et al., 2015; Zhang et al., 2014), and low wind speed over the coast can be one of the reasons that limit gas transfer modulation over coastal waters (Gutiérrez-Loza & Ocampo-Torres, 2016).

High-accuracy measurements of CO_2 flux on coastal waters is essential in understanding the global carbon processes and accuracy of future projection studies of carbon sources and sequestration. So, the application of the WPL correction to CO_2 flux measurements over the coastal waters must be investigated. Therefore, the objective of this paper is to assess the WPL correction method on CO_2 flux measurement at a tropical coastal water location.

2. Materials and Methods

2.1 The EC Dataset

This analysis uses the *in-situ* EC data collected from an automated weather station called the "Muka Head Station" in the Centre for Marine and Coastal Studies of Universiti Sains Malaysia. The station is located on the northwestern part of Penang, Peninsular Malaysia at 5°28′06"N, 100°12′01"E (see Figure 1a).

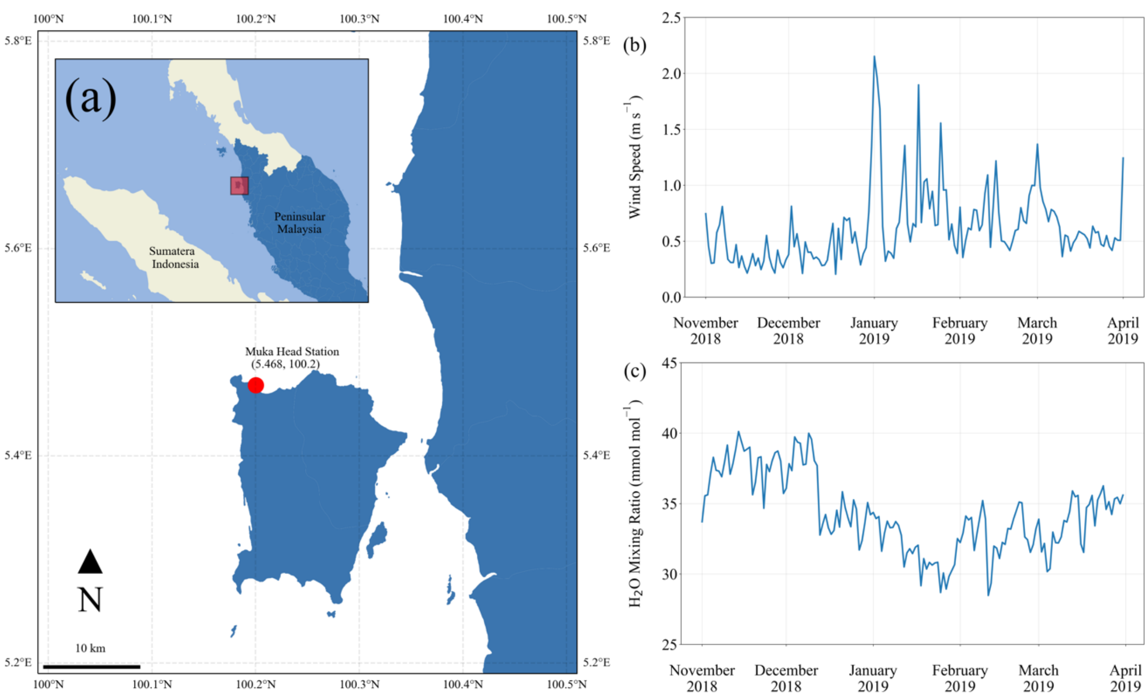

Figure 1 (a) Red circle and box show the location of the automated weather station called the Muka Head Station in Penang, Peninsular Malaysia; (b) the daily-averaged wind speed; (c) the daily-averaged H_2O mixing ratio during the Northeast Monsoon.

Based on Figure 1b, the range of wind speeds in the study location during the Northeast Monsoon is between 0.20 m s^{-1} and 2.15 m s^{-1}, while the average is 0.61 m s^{-1}, which is lower than the coast study area of Gutiérrez-Loza and Ocampo-Torres (2016). Furthermore, the H_2O mixing ratio (refer Figure 1c) has an average of 34.31 mmol mol^{-1}, with a minimum of 28.47 mmol mol^{-1} and a maximum of 40.12 mmol mol^{-1}. Meanwhile, the range of salinity values is relatively low, with a minimum of 32.74 °/oo, a maximum of 34.1 °/oo, and an average of 33.43 °/oo since the site is located over the coast in the tropics, where the salinity is naturally low and does not vary much (Zhu et al., 2009). Overall, the data suggest that there is a relatively low level of salinity and wind speeds.

The station measures CO_2 and H_2O fluxes and bio-meteorological parameters (global radiation, net radiation, seawater temperature, etc.) of a tropical coastal ocean in the Strait of Malacca. The flux is calculated from the 20-Hz data collected by the open-path LI-7500 infrared CO_2/H_2O analyzer (LI-COR, USA) and a sonic anemometer (RM81000, Young, USA). The site is exposed to minimal anthropogenic influence. Other details of the instrumentation can be seen in the published literature (Yusup et al., 2020).

From the entire list of variables available in the dataset, the primary variable analyzed was the EC's CO_2 flux. The data is accessible at http://atmosfera.usm.my and has a time resolution of 30 minutes. The duration of the dataset was from 2015 until 2023, however, the temporal scope of this analysis is five months. The months sampled are in the Northeast Monsoon (November 2018 – March 2019). Analyses and plots were performed and generated using Python ver. 3.9.

2.2 Calculations of the Raw, WPL-Corrected, and Standard CO_2 Fluxes

The CO_2 flux is calculated "raw" using the EC technique. The method applies the vertical turbulence exchange concept to calculate the flux directly by using the vertical wind velocity, molar density of dry air, and the mixing ratio of CO_2 (Aubinet et al., 2000). The EC method uses Equation (1).

$$F_{c,raw} = \overline{\rho_a}\,\overline{w'c'} \qquad (1)$$

F_c is CO_2 flux, ρ_a is molar density of dry air, w is vertical component of wind speed, and c is dry air mixing ratio of CO_2.

The WPL correction method is applied to the raw CO_2 flux calculated using Equation (1). The WPL formula is shown in Equation (2).

$$F_{c,WPL} = \overline{w'\rho_c'} + (1+\mu\sigma)\frac{\overline{\rho_c}}{\overline{T}}\overline{w'T'} + \mu\frac{\overline{\rho_c}}{\overline{\rho_a}}\overline{w'\rho_v'} + (1+\mu\sigma)\frac{\overline{\rho_c}}{\overline{P}}\overline{w'P'} \quad (2)$$

T is temperature, P is pressure, ρ_c is molar density of CO_2, ρ_v is molar density of water vapor, ρ_a is molar density of dry air (Webb et al., 1980). Meanwhile, $\sigma = \rho_v/\rho_a$ and $\mu = M_a/M_v$ with M_a is molecular weight of dry air, M_v is molecular weight of water vapor. The WPL formula consists of the corrections for temperature, water vapor, and pressure fluctuations in the open-path gas analyzer, which are stated in the second, third, and fourth terms in the Equation 2. The first term on the right section of WPL formula is CO_2 flux of EC method that has not been corrected.

The WPL-corrected CO_2 flux ($F_{c,WPL}$) is compared to the raw CO_2 flux ($F_{c,raw}$) and the standard-calculated CO_2 flux ($F_{c,std}$). $F_{c,std}$ is the CO_2 flux that incorporates other corrections in addition to the WPL correction: 1) wind speed movement offsets, 2) spectral correction of low-pass filtering and high-pass filtering. The methods used to calculate $F_{c,std}$ flux are similar to those utilized in the widely used flux processing software, EddyPro® (ver. 7, LI-COR, USA). In this research, $F_{c,std}$ was used to serve as a benchmark to analyze the application of the WPL correction.

2.3 Performance Metrics

The comparison among the fluxes calculated involves the correlation among the $F_{c,raw}$, $F_{c,WPL}$, and $F_{c,std}$. This analysis used the Pearson correlation coefficient, which determines the degree of linearity between two quantitative variables and expresses the degree of relationship between them. The coefficient can be positive or negative, depending on the direction of correspondence between changes in the two variables.

In addition, the evaluation metrics of Root Mean Squared Error (RMSE) and Mean Absolute Error (MAE) were used to measure the magnitude of the error of $F_{c,raw}$ and $F_{c,WPL}$ compared to $F_{c,std}$. The RMSE takes the square root of the average of squared differences to measure the average magnitude of the error, while the MAE calculates the average of the absolute differences between two values to measure the average magnitude of the errors without considering the direction (positive or negative).

3. Results and Discussion

3.1 The $F_{c,std}$ Hourly Cycle at the Tropical Coast

Throughout the sampling time domain, $F_{c,std}$ was generally negative, which exhibited that the tropical coast was a CO_2 sink. It is important to note that the sampling domain is in the Northeast Monsoon, which is known to be a period of strong upwelling processes (Gayathri et al., 2022; Mandal et al., 2021; Tan et al., 2006). The magnitude of the negative CO_2 flux varied with the hours (Figure 2a), but it averaged to –0.10 μmol m^{-2} s^{-1}. In the diel cycle, the lowest negative flux occurred during the daytime, with the flux closing to equilibrium at around 14:00 LT. Meanwhile, the CO_2 flux during the nighttime displayed greater uptake movements, with the lowest peak occuring at 06:00 LT.

This diel cycle is similar to the CO_2 flux trend reported in the Rey–Sánchez et al. (2017) study as carbon uptake, which was conducted at the coastal waters of the Gulf of Aqaba, Israel. Of note is the flux magnitude of this site is lower by 90.48% than the cited study's flux (–1.05 μmol m^{-2} s^{-1}). The similarities can be seen in the trend of negative CO_2 fluxes, which reduced towards equilibrium at 12:00 LT from 06:00 LT; similarly, greater CO_2 uptake occurred during the night.

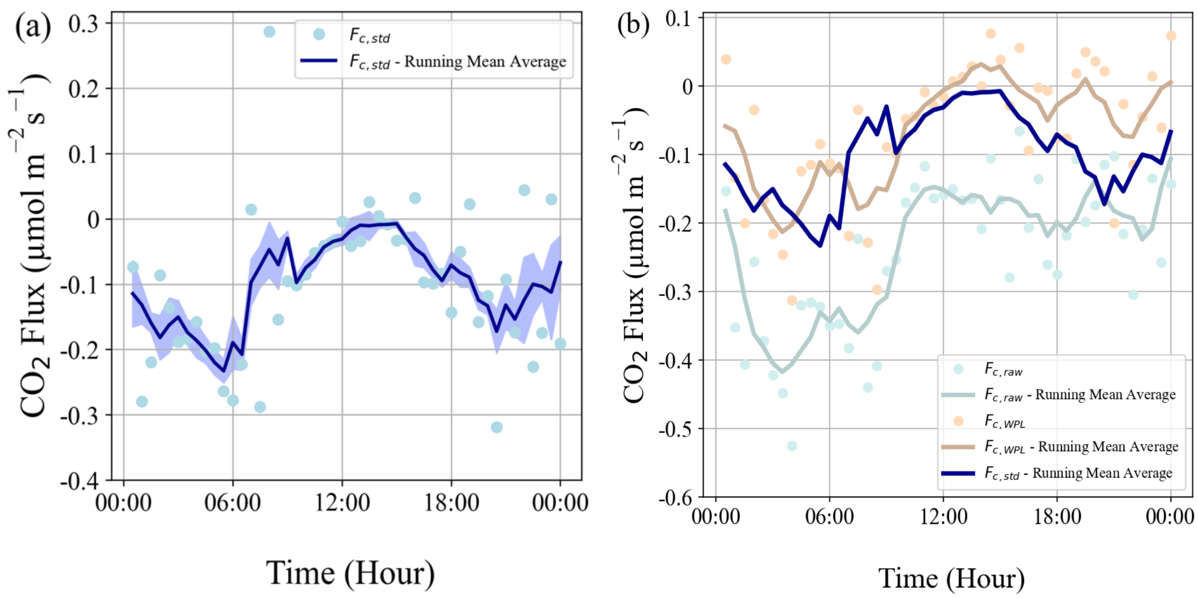

Figure 2 (a) The hourly trend of $F_{c,std}$ and its running-mean average at the tropical coast; (b) the hourly trends of $F_{c,raw}$, $F_{c,WPL}$, and $F_{c,std}$ and their running-mean average.

Figure 2a also displays the standard error of the $F_{c,std}$, indicating a notable level of uncertainty during the morning and evening, but a lower level from 09:00 LT until in the afternoon. On average, the standard error measures 0.02 μmol m^{-2} s^{-1}, ranging from a minimum of 0.005 μmol m^{-2} s^{-1} to a maximum of 0.07 μmol m^{-2} s^{-1}. The observed high uncertainty during specific times may be attributed to fluctuations in evaporation. For instance, an increase in the uncertainty to 0.04 μmol m^{-2} s^{-1} at 08:00 LT was observed due to quite intense fluctuations in evaporation around that time, which may have influenced the CO_2 flux's uncertainty.

3.2 Values and Trends Comparison among the $F_{c,raw}$, $F_{c,WPL}$, and $F_{c,std}$

The average values of $F_{c,raw}$ and $F_{c,WPL}$ are –0.25 and –0.07 μmol m^{-2} s^{-1}, respectively, and both display negative fluxes (refer Figure 2b), which is the same as $F_{c,std}$. The decrease of these three fluxes typically was observed between 06:00 LT and 12:00 LT. The lower flux magnitudes can be attributed to the decrease in wind speed during this period, which lowers the transfer velocity and reduces CO_2 flux in accordance with the bulk formula (Wanninkhof, 1992; Wanninkhof et al., 2009).

There is a varying trend between $F_{c,raw}$ and $F_{c,WPL}$ with $F_{c,std}$. $F_{c,raw}$ and $F_{c,WPL}$ show a significant increase after 00:00 LT, while $F_{c,std}$ increases significantly after 12:00 LT, with another increase occurring from 00:00 LT to 06:00 LT following a decrease before 00:00 LT. The CO_2 flux diel cycle reported by Rey-Sánchez et al. (2017) is more similar to $F_{c,raw}$ and $F_{c,WPL}$ fluxes than to $F_{c,std}$.

The average value of $F_{c,std}$ is significantly lower (higher) than the $F_{c,raw}$ ($F_{c,WPL}$) by –60% (+46%). The difference can be due to the application of correction methods in addition to the WPL correction. According to LI-COR (2021), wind speed measurement offsets and spectral corrections, such as low-pass and high-pass filtering, are necessary in estimating CO_2 flux. The absence of these corrections caused the $F_{c,WPL}$ to be lower, on average magnitude, than the $F_{c,std}$.

Between $F_{c,raw}$ and $F_{c,WPL}$, $F_{c,WPL}$ is lower than $F_{c,raw}$ by 0.17 μmol m^{-2} s^{-1}. This result is the same as the observation on the open sea by Kondo and Tsukamoto (2007), albeit the magnitude difference in this research is not as significant as theirs. For instance, the magnitude difference by the WPL correction in the cited study is higher by 1.40 μmol m^{-2} s^{-1}. The large difference in the latter study was accompanied by a higher average magnitude of the $F_{c,raw}$ reaching up to 1.42 μmol m^{-2} s^{-1}, which can be due to the location of their study, i.e., the open sea with strong winds. On average, the $F_{c,WPL}$ is much lower than the $F_{c,raw}$ flux by >70%–98% for both over the sea and the coastal waters, but it will result in a CO_2 flux value being close to the $F_{c,std}$ as well as CO_2 flux calculated using the bulk transfer equation as measured in Kondo and Tsukamoto (2007). Thus, despite the deviation, the WPL correction still serves its purpose in reducing the overestimation of CO_2 flux collected by the open-path gas analyzers.

The resulting correlations also highlights the difference in CO_2 flux after applying the WPL correction (see Figure 3). It shows that the correlation of the $F_{c,std}$ and $F_{c,raw}$ (refer Figure 3a) as well as the correlation of the $F_{c,std}$ and $F_{c,WPL}$ (refer Figure 3b) are strong and similar. The correlation between $F_{c,WPL}$ and $F_{c,std}$ is slightly lower than the correlation between $F_{c,raw}$ and $F_{c,std}$, i.e., 0.75 and 0.76, respectively. Moreover, the CO_2 flux trend between the $F_{c,raw}$ and $F_{c,WPL}$ is somewhat the same with a very strong correlation (r = 0.96) as shown in Figure 3c. It must be pointed out that the lower correlation level between $F_{c,WPL}$ and $F_{c,std}$ does not indicate that the WPL correction reduces the accuracy of the CO_2 flux estimation.

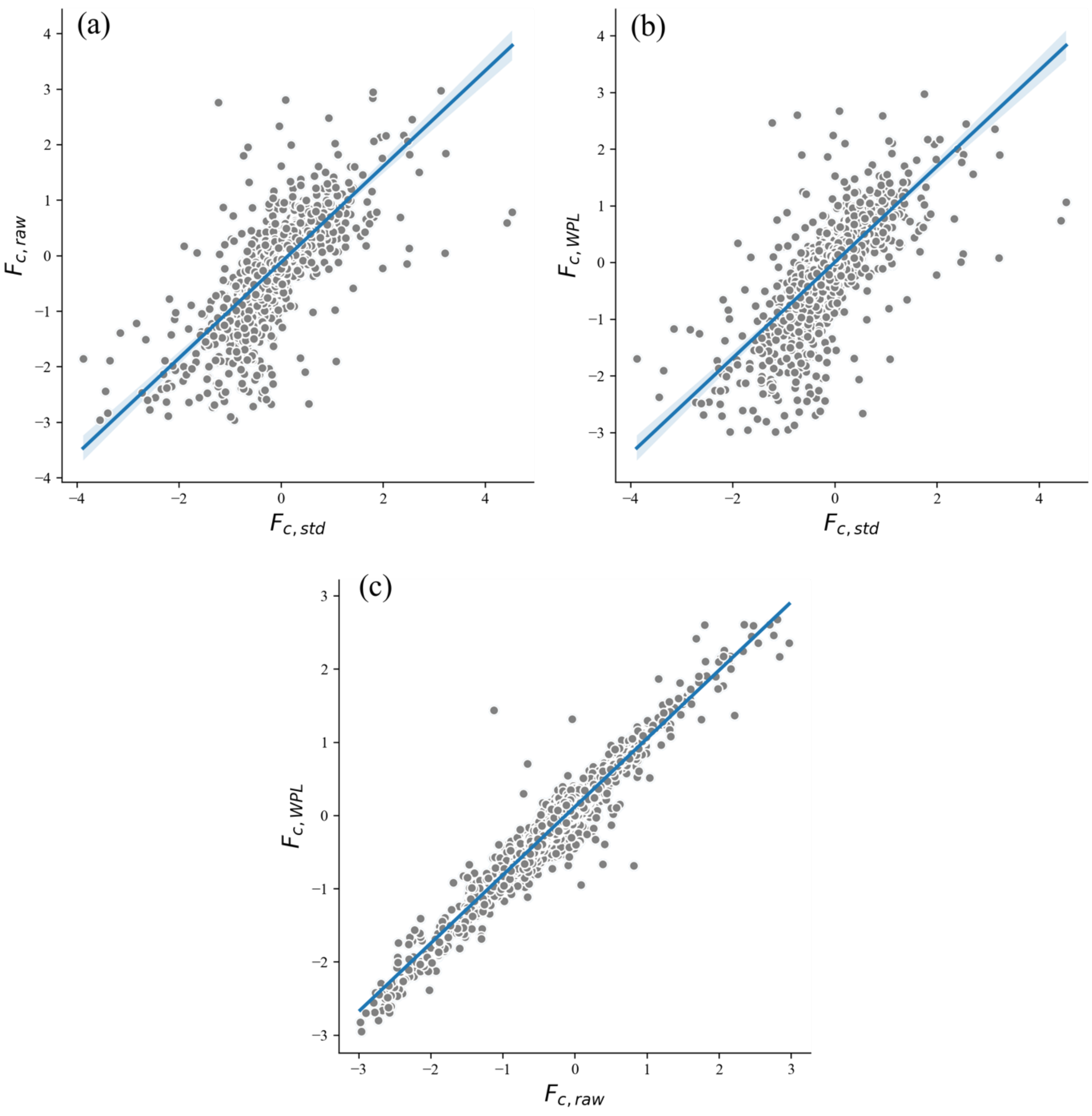

Figure 3 The scatter plots for (a) $F_{c,raw}$ and $F_{c,std}$, (b) $F_{c,WPL}$ and $F_{c,std}$, and (c) $F_{c,raw}$ and $F_{c,WPL}$.

The RMSE values for $F_{c,raw}$ and $F_{c,WPL}$ were found to be 0.35 μmol m^{-2} s^{-1} and 0.33 μmol m^{-2} s^{-1}, respectively, in comparison to $F_{c,std}$. This suggests that the WPL correction reduces the overall error magnitude, resulting in a more accurate estimation of the CO_2 flux. Moreover, the

MAE for $F_{c,WPL}$ (0.18 µmol m^{-2} s^{-1}) is also lower than the MAE for $F_{c,raw}$ (0.20 µmol m^{-2} s^{-1}) when compared to $F_{c,std}$. This implies that the WPL correction not only reduces the overall error magnitude but also improves the accuracy of the estimated CO_2 flux.

Nevertheless, the WPL correction also produced positive CO_2 flux several times in the afternoon and the evening, whereas the $F_{c,raw}$ only showed negative fluxes as shown in Figure 2b. For instance, a sign change occurred at 13:30 LT with an $F_{c,raw}$ value of –0.16 µmol m^{-2} s^{-1} and an $F_{c,WPL}$ value of 0.03 µmol m^{-2} s^{-1}. At 16:00 LT, there was also a sign change as the $F_{c,raw}$ value is –0.11 µmol m^{-2} s^{-1} but the $F_{c,WPL}$ value is 0.02 µmol m^{-2} s^{-1}. The different results, particularly in the change of the negative sign to the positive sign of the CO_2 flux, can drastically change the conclusion of the carbon exchange in the studied location. Thus, the WPL correction needs to be implemented conscientiously to achieve a more meaningful CO_2 flux measurement.

3.3 Positive-Negative Sign Change of the CO_2 Flux Due to WPL Correction

Based on $F_{c,std}$, the tropical coast acted as CO_2 uptake, particularly in January 2019. The $F_{c,std}$ has an average of –0.10 µmol m^{-2} s^{-1}, with a similar range of magnitude throughout the Northeast Monsoon; note that the Northeast Monsoon transpire between November and March, annually. The magnitude of $F_{c,std}$ in January also increased in the afternoon, which is the same as the $F_{c,std}$ in other months in the Northeast Monsoon.

Compared to the CO_2 flux diel cycle in the Northeast Monsoon, the flux in January exhibited a different characteristic than the other months of the monsoon (refer Figure 4). The difference is apparent in the magnitude of the $F_{c,std}$ in January; it started to decrease again before 00:00 LT unlike in other months (see section 3.1). Subsequently, the flux in January fluctuated close to equilibrium longer until after 15:00 LT. The difference in the characteristics of the CO_2 flux in January can be interpreted as the monthly variability of meteorological and oceanographic parameters that caused different CO_2 flux responses.

Based on the CO_2 flux in January (refer Figure 4), the $F_{c,WPL}$ is also lower than the $F_{c,raw}$, confirming the same results of applying the WPL formula in terms of underestimation. The absolute average value of the $F_{c,WPL}$ in this month is lower than the $F_{c,raw}$ by 93%. Meanwhile, the $F_{c,std}$ is lower than the $F_{c,raw}$ by 47% but higher than the absolute $F_{c,WPL}$ by a factor of 75. The spectral correction methods of the low-pass and high-pass filtering corrections implemented in the $F_{c,std}$ appears to prevent the underestimation from resulting a sign change of the flux.

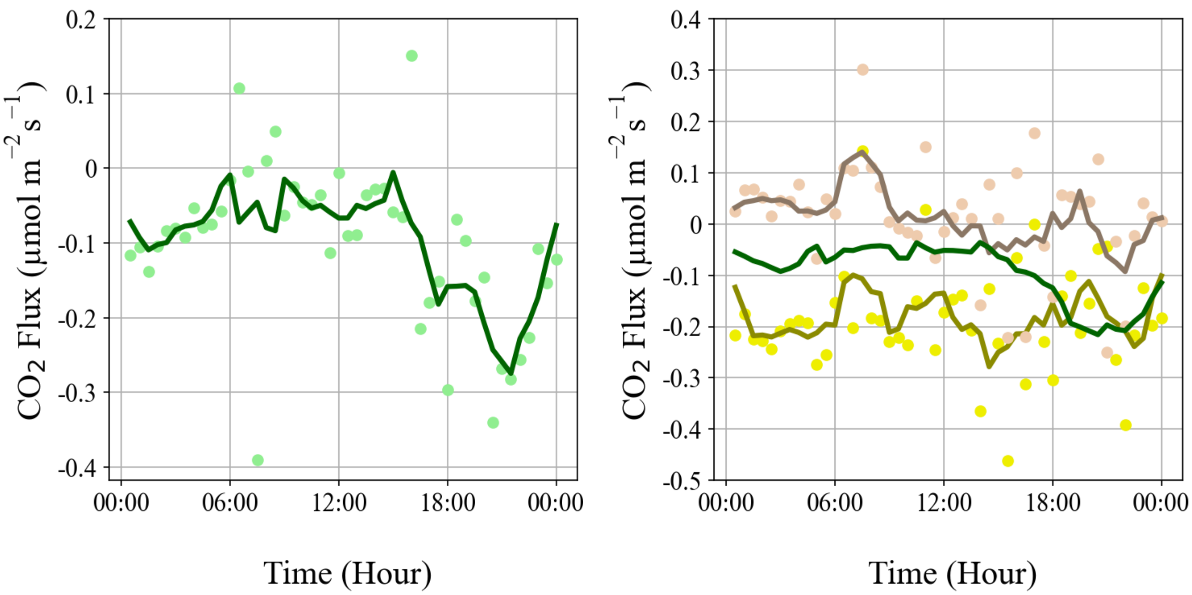

Figure 4 The hourly trend CO_2 flux for $F_{c,std}$ (left panel) as well as $F_{c,raw}$ and $F_{c,WPL}$ (right panel) in January 2019. The yellow, brown, and green colors represent $F_{c,raw}$ and $F_{c,WPL}$, and $F_{c,std}$, respectively. The line is the hourly averaged trend of each $F_{c,raw}$ and $F_{c,WPL}$, and $F_{c,std}$.

Between $F_{c,raw}$ and $F_{c,WPL}$, the CO_2 flux calculated using the WPL formula displays a pattern that more closely resembled the $F_{c,std}$. The $F_{c,WPL}$ pattern showed a greater magnitude flux during evening and lower magnitude flux in the morning until afternoon.

More importantly, the flux underestimation caused by the WPL formula resulted in a changing positive-negative sign of the average CO_2 flux. The average for $F_{c,raw}$ is –0.19 μmol m^{-2} s^{-1}, whereas the average for the $F_{c,WPL}$ flux is 0.014 μmol m^{-2} s^{-1}. Compared to the Northeast Monsoon, the average value of $F_{c,raw}$ in January is lower, which suggests that the likelihood of a sign change increases when the CO_2 flux is lower or closer to equilibrium. Moreover, Figure 4 shows there are more positive CO_2 flux from 00:00 LT to 12:00 LT for $F_{c,WPL}$. Hence, the WPL correction causes the negative average value of the $F_{c,raw}$ to change to a positive average value, which indicate the change in the role of the coast as a source or sink of CO_2.

The WPL correction formula indicates that the measurement of $F_{c,raw}$ is higher in value and should be corrected for temperature, water vapor, and pressure fluctuations. The largest correction values are attributed to temperature and water vapor fluctuations, which averaged to 10^{-6} and 10^{-4} μmol m^{-2} s^{-1}, respectively. In contrast, the correction for pressure fluctuations has the least significant effect, the difference in average values is a factor of 10^{300}. Consequently, temperature and water vapor corrections are the most influential factors in altering the sign of CO_2 flux when applying the WPL correction.

4 Conclusions

The WPL formula was introduced to improve the accuracy of CO_2 flux measurement using the EC method. In this research, the WPL correction was applied on the CO_2 flux measured over the tropical coastal waters to compare the performance of the correction. Three flux calculation methods were evaluated: 1) standard (including WPL and other correction methods), 2) raw, and 3) WPL. The $F_{c,std}$ is lower than $F_{c,raw}$ by 60% but is higher than $F_{c,WPL}$ by 46%, which can be due to additional corrections applied to $F_{c,std}$. The $F_{c,WPL}$ (–0.07 μmol m^{-2} s^{-1}) is lower than $F_{c,raw}$ (–0.25 μmol m^{-2} s^{-1}) by an average of 0.17 μmol m^{-2} s^{-1}. The WPL correction and the standard method produced a clearer hourly CO_2 flux trend than the raw calculated flux. Overall, the WPL formula produces a lower magnitude flux than the uncorrected CO_2 flux by over 70%, serving its purpose in minimizing the CO_2 flux overestimation. However, the temperature and water vapor fluctuations terms in the WPL correction have the greatest impact on altering the positive-negative sign of CO_2 flux. Therefore, the WPL correction needs to be implemented conscientiously to obtain a more accurate CO_2 flux using the EC technique over the tropical coast. Further research is needed to quantify the uncertainty associated with the sign change.

Acknowledgements

We acknowledge that the Malaysian Research University Network Long-Term Research Grant Scheme (MRUN-LRGS), with grant number 203.PTEKIND.6777006, from the Ministry of Education Malaysia, enabled us to conduct this research. Additionally, we express our gratitude towards Elite Scientific Instruments Sdn. Bhd., our industry partner, for their contribution of sensors that allowed us to take accurate measurements.

Open Research

The data used in the study was obtained from the Muka Head Station in the Centre for Marine and Coastal Studies of Universiti Sains Malaysia, it and can be accessed at http://atmosfera.usm.my/api.html (Yusup & Sigid, 2023). The maps used in the study were created through Cartopy version 0.19.0 (Elson et al., 2021), which is a library for creating maps and geospatial data visualizations. Cartopy can be accessed at https://scitools.org.uk/cartopy/docs/latest/. The figures were created using Matplotlib version 3.5.1 (Caswell et al., 2021; Hunter, 2007), which is a tool for creating graphs and plots. Matplotlib is available under the Matplotlib license at https://matplotlib.org/.

References

Aalto, N. J., Campbell, K., Eilertsen, H. C., & Bernstein, H. C. (2021). Drivers of Atmosphere-Ocean CO2 Flux in Northern Norwegian Fjords. *Frontiers in Marine Science*, *8*. https://doi.org/10.3389/fmars.2021.692093

Aubinet, M., Grelle, A., Ibrom, A., Rannik, Ü., Moncrieff, J., Foken, T., Kowalski, A. S., Martin, P. H., Berbigier, P., Bernhofer, Ch., Clement, R., Elbers, J., Granier, A., Grünwald, T., Morgenstern, K., Pilegaard, K., Rebmann, C., Snijders, W., Valentini, R., & Vesala, T. (2000). *Estimates of the Annual Net Carbon and Water Exchange of Forests: The EUROFLUX Methodology*.

Borges, A. v., Delille, B., & Frankignoulle, M. (2005). Budgeting sinks and sources of CO2 in the coastal ocean: Diversity of ecosystem counts. *Geophysical Research Letters*, *32*(14), 1–4. https://doi.org/10.1029/2005GL023053

Broecker, W. S., Ledwell, J. R., Takahashi, T., Weiss, R., Merlivat, L., Memery, L., Peng, T.-H., Jahne, B., & Munnich, K. O. (1986). Isotopic versus micrometeorologic ocean CO 2 fluxes: A serious conflict . *Journal of Geophysical Research*, *91*(C9), 10517. https://doi.org/10.1029/jc091ic09p10517

Burba, G., Madsen, R., & Feese, K. (2013). Eddy covariance method for CO2 emission measurements in CCUS applications: Principles, instrumentation and software. *Energy Procedia*, *40*, 329–336. https://doi.org/10.1016/j.egypro.2013.08.038

Caswell, T. A., Droettboom, M., Lee, A., Sales De Andrade, E., Hoffmann, T., Hunter, J., Klymak, J., Firing, E., Stansby, D., Varoquaux, N., Hedegaard Nielsen, J., Root, B., May, R., Elson, P., Seppänen, J. K., Dale, D., Lee, J.-J., McDougall, D., Straw, A., … Ivanov, P. (2021). *matplotlib/matplotlib: REL: v3.5.1*. Zenodo. https://doi.org/10.5281/zenodo.5773480

Chien, H., Zhong, Y. Z., Yang, K. H., & Cheng, H. Y. (2018). Diurnal variability of CO2 flux at coastal zone of Taiwan based on eddy covariance observation. *Continental Shelf Research*, *162*, 27–38. https://doi.org/10.1016/j.csr.2018.04.006

Doney, S. C., Tilbrook, B., Roy, S., Metzl, N., le Quéré, C., Hood, M., Feely, R. A., & Bakker, D. (2009). Surface-ocean CO2 variability and vulnerability. *Deep-Sea Research Part II: Topical Studies in Oceanography*, *56*(8–10), 504–511. https://doi.org/10.1016/j.dsr2.2008.12.016

Edson, J. B., Fairall, C. W., Bariteau, L., Zappa, C. J., Cifuentes-Lorenzen, A., McGillis, W. R., Pezoa, S., Hare, J. E., & Helmig, D. (2011). Direct covariance measurement of CO2 gas transfer velocity during the 2008 Southern Ocean Gas Exchange Experiment: Wind speed dependency. *Journal of Geophysical Research: Oceans*, *116*(11). https://doi.org/10.1029/2011JC007022

Else, B. G. T., Papakyriakou, T. N., Galley, R. J., Drennan, W. M., Miller, L. A., & Thomas, H. (2011). Wintertime CO2 fluxes in an Arctic polynya using eddy covariance: Evidence for enhanced air-sea gas transfer during ice formation. *Journal of Geophysical Research: Oceans*, *116*(9). https://doi.org/10.1029/2010JC006760

Elson, P., de Andrade, E. S., Hattersley, R., May, R., Lucas, G., Campbell, E., Dawson, A., Raynaud, S., scmc72, Little, B., Donkers, K., Blay, B., Killick, P., Wilson, N., Peglar, P., lbdreyer, Andrew, Szymaniak, J., Berchet, A., … Bindle, L. (2021). *SciTools/cartopy: v0.19.0*. Zenodo. https://doi.org/10.5281/zenodo.4707961

Gayathri, N. M., Sijinkumar, A. v, Nath, B. N., Sandeep, K., & Wei, K. Y. (2022). A ~ 30 kyr sub-centennial to millennial Indian summer monsoon variability record from the southern Andaman Sea, northeastern Indian Ocean. *Palaeogeography, Palaeoclimatology, Palaeoecology*, *590*, 110865. https://doi.org/https://doi.org/10.1016/j.palaeo.2022.110865

Gutiérrez-Loza, L., & Ocampo-Torres, F. J. (2016). Air-sea CO2 fluxes measured by eddy covariance in a coastal station in Baja California, México. *IOP Conference Series: Earth and Environmental Science*, *35*(1). https://doi.org/10.1088/1755-1315/35/1/012012

He, Y., Yang, J., Zhuang, Q., Harden, J. W., McGuire, A. D., Liu, Y., Wang, G., & Gu, L. (2015). Incorporating microbial dormancy dynamics into soil decomposition models to improve quantification of soil carbon dynamics of northern temperate forests. *Journal of Geophysical Research: Biogeosciences*, *120*(12), 2596–2611. https://doi.org/10.1002/2015JG003130

Heimsch, L., Lohila, A., Tuovinen, J. P., Vekuri, H., Heinonsalo, J., Nevalainen, O., Korkiakoski, M., Liski, J., Laurila, T., & Kulmala, L. (2021). Carbon dioxide fluxes and carbon balance of an agricultural grassland in southern Finland. *Biogeosciences*, *18*(11), 3467–3483. https://doi.org/10.5194/bg-18-3467-2021

Horst, T. W. (1997). *A simple formula for attenuation of eddy fluxes measured with first-order-response scalar sensors*.

Hunter, J. D. (2007). Matplotlib: A 2D Graphics Environment. *Computing in Science & Engineering*, *9*(3), 90–95. https://doi.org/10.1109/MCSE.2007.55

Ikawa, H., Faloona, I., Kochendorfer, J., Paw U, K. T., & Oechel, W. C. (2013). Air-sea exchange of CO2 at a Northern California coastal site along the California Current upwelling system. *Biogeosciences*, *10*(7), 4419–4432. https://doi.org/10.5194/bg-10-4419-2013

Jones, E. P., & Smith, S. D. (1977). A first measurement of sea-air CO 2 flux by eddy correlation . *Journal of Geophysical Research*, *82*(37), 5990–5992. https://doi.org/10.1029/jc082i037p05990

K Webb, B. E., Pearman, G. I., & Leuning, R. (1980). *Correction of flux measurements for density effects due to heat and water vapour transfer* (Vol. 106).

Kondo, F., & Tsukamoto, O. (2007). Air-Sea CO 2 Flux by Eddy Covariance Technique in the Equatorial Indian Ocean. In *Journal of Oceanography* (Vol. 63).

LI-COR. (2021). *EddyPro Software Instruction Manual*.

Lokupitiya, E., Denning, A. S., Schaefer, K., Ricciuto, D., Anderson, R., Arain, M. A., Baker, I., Barr, A. G., Chen, G., Chen, J. M., Ciais, P., Cook, D. R., Dietze, M., el Maayar, M., Fischer, M., Grant, R., Hollinger, D., Izaurralde, C., Jain, A., … Xue, Y. (2016). Carbon and energy fluxes in cropland ecosystems: a model-data comparison. *Biogeochemistry*, *129*(1–2), 53–76. https://doi.org/10.1007/s10533-016-0219-3

Mandal, S., Behera, N., Gangopadhyay, A., Susanto, R. D., & Pandey, P. C. (2021). Evidence of a chlorophyll "tongue" in the Malacca Strait from satellite observations. *Journal of Marine Systems*, *223*. https://doi.org/10.1016/j.jmarsys.2021.103610

Massman, W. J. (2000). A simple method for estimating frequency response corrections for eddy covariance systems. In *Agricultural and Forest Meteorology* (Vol. 104).

Massman, W. J. (2001). Reply to comment by Rannik on "A simple method for estimating frequency response corrections for eddy covariance systems." In *Agricultural and Forest Meteorology* (Vol. 107).

McGowan, H. A., MacKellar, M. C., & Gray, M. A. (2016). Direct measurements of air-sea CO2 exchange over a coral reef. *Geophysical Research Letters*, *43*(9), 4602–4608. https://doi.org/10.1002/2016GL068772

Moncrieff, J. B., Massheder, J. M., de Bruin, H., Elbers, J., Friborg, T., Heusinkveld, B., Kabat, P., Scott, S., Soegaard, H., & Verhoef, A. (1997). A system to measure surface fluxes of momentum, sensible heat, water vapour and carbon dioxide. In *Journal of Hydrology ELSEVIER Journal of Hydrology*.

Nakai, Y., Matsuura, Y., Kajimoto, T., Abaimov, A. P., Yamamoto, S., & Zyryanova, O. A. (2008). Eddy covariance CO2 flux above a Gmelin larch forest on continuous permafrost in Central Siberia during a growing season. *Theoretical and Applied Climatology*, *93*(3–4), 133–147. https://doi.org/10.1007/s00704-007-0337-x

Prytherch, J., Yelland, M. J., Pascal, R. W., Moat, B. I., Skjelvan, I., & Neill, C. C. (2010). Direct measurements of the CO2 flux over the ocean: Development of a novel method. *Geophysical Research Letters*, *37*(3). https://doi.org/10.1029/2009GL041482

Prytherch, J., Yelland, M. J., Pascal, R. W., Moat, B. I., Skjelvan, I., & Srokosz, M. A. (2010). Open ocean gas transfer velocity derived from long-term direct measurements of the CO2 flux. *Geophysical Research Letters*, *37*(23). https://doi.org/10.1029/2010GL045597

Rey-Sánchez, A. C., Bohrer, G., Morin, T. H., Shlomo, D., Mirfenderesgi, G., Gildor, H., & Genin, A. (2017). Evaporation and CO2 fluxes in a coastal reef: an eddy covariance approach. *Ecosystem Health and Sustainability*, *3*(10). https://doi.org/10.1080/20964129.2017.1392830

Stull, R. B. (1988). *An Introduction to Boundary Layer Meteorology*. https://doi.org/https://doi.org/10.1007/978-94-009-3027-8

Tan, J. C. H., Peters, D. M., & Kaufman, P. L. (2006). Recent developments in understanding the pathophysiology of elevated intraocular pressure. *Current Opinion in Ophthalmology*, *17*(2), 168–174. https://doi.org/10.1016/j.csr.2005.09.008

Tokoro, T., & Kuwae, T. (2018). Improved post-processing of eddy-covariance data to quantify atmosphere-aquatic ecosystem CO2 Exchanges. *Frontiers in Marine Science*, *5*(AUG). https://doi.org/10.3389/fmars.2018.00286

Wanninkhof, R. (1992). Relationship Between Wind Speed and Gas Exchange Over the Ocean. In *JOURNAL OF GEOPHYSICAL RESEARCH* (Vol. 97, Issue C5).

Wanninkhof, R., Asher, W. E., Ho, D. T., Sweeney, C., & McGillis, W. R. (2009). Advances in quantifying air-sea gas exchange and environmental forcing. In *Annual Review of Marine Science* (Vol. 1, pp. 213–244). https://doi.org/10.1146/annurev.marine.010908.163742

Webb, E. K., Pearman, G. I., & Leuning, R. (1980). *Correction of flux measurements for density effects due to heat and water vapour transfer* (Vol. 106).

Yang, M., Prytherch, J., Kozlova, E., Yelland, M. J., Parenkat Mony, D., & Bell, T. G. (2016). Comparison of two closed-path cavity-based spectrometers for measuring air-water CO2 and CH4 fluxes by eddy covariance. *Atmospheric Measurement Techniques*, *9*(11), 5509–5522. https://doi.org/10.5194/amt-9-5509-2016

Yusup, Y., Ramli, N. K., Kayode, J. S., Yin, C. S., Hisham, S., Isa, H. M., & Ahmad, M. I. (2020). Atmospheric carbon dioxide and electricity production due to lockdown. *Sustainability (Switzerland)*, *12*(22), 1–12. https://doi.org/10.3390/su12229397

Yusup, Y., & Sigid, M. F. (2023). *Assessing the Webb-Pearman-Leuning Formula in Estimating CO2 Flux at a Tropical Coast*. https://doi.org/10.6084/m9.figshare.22139939.v1

Zhang, H. F., Chen, B. Z., van der Laan-Luijkx, I. T., Chen, J., Xu, G., Yan, J. W., Zhou, L. X., Fukuyama, Y., Tans, P. P., & Peters, W. (2014). Net terrestrial CO2 exchange over China during 2001–2010 estimated with an ensemble data assimilation system for atmospheric CO2.

Journal of Geophysical Research, *119*(6), 3500–3515. https://doi.org/10.1002/2013JD021297

Zhu, Y., Shang, S., Zhai, W., & Dai, M. (2009). Satellite-derived surface water pCO2 and air-sea CO2 fluxes in the northern South China Sea in summer. *Progress in Natural Science*, *19*(6), 775–779. https://doi.org/10.1016/j.pnsc.2008.09.004